

Coupling of the Wave Equation and a Hanging Cable

Sofia Iannicelli, Nicole Peterson

Mechanical Engineering Department
Brigham Young University
Provo, Utah 84602
{isofiag, nap36}@byu.edu

Abstract

We examine interaction between the wave equation and a hanging cable. Specifically, we drive the motion of the hanging cable from the wave equation and observe the results. We use D'Alembert's solution to the spatially unbounded wave equation. We derive the equation for the hanging cable via a custom integral transform and the Laplace transform. The cable is bounded at one end by the values of the wave equation, coupling the two systems together. Code and sample simulation results can be found at <https://github.com/sofia-i/me505-paper>.

Nomenclature

For the infinite wave system:

- $\nu(x, t)$: infinite 'wind' function
- v : wave propagation speed
- ν_0, ν_1 initial conditions

For the hanging cable:

- $u(\varphi, t)$: finite hanging cable
- w : propagation speed
- L : domain upper limit

Note: to differentiate the spatial domains, we use x for the wave's spatial domain and φ for the chain's spatial domain.

Introduction

The simulation of hair and strand-like structures is a well-known challenge in computer graphics and other applications. One interesting subject area in hair simulation is coupling a hair solver with a solver of a different type; for example, simulating wet hair requires coupling a hair simulator with a fluid solver. In this paper, we examine the influence of a wave on a cable, strand-like structure.

Coupling refers to interaction between systems. The interactions of various systems or behaviors can be observed and simulated by coupling multiple elements; for example, mass-spring-damper models in mechanical engineering can combine multiple distinct elements—including forcing or driving functions—into a single differential equation. In animation, complex phenomena such as hairs interacting with water can be simulated via coupled solvers.

Methodology

The wind was approximated using the wave equation; while this is not strictly accurate since the wave function

is intended to describe motion in a medium such as water, it provides a sufficient approximation for visualization. Boundary conditions were not defined for the wave equation, as the wind was assumed to be spatially infinite.

D'Alembert's solution [5], which solves for the wave equation without boundary conditions, was used to find the function defining this wave:

$$\nu(x, t) = \frac{1}{2}[\nu_0(x - vt) + \nu_0(x + vt)] + \frac{1}{2v} \int_{x-vt}^{x+vt} \nu_1(s) ds \quad (1)$$

We set the initial conditions as follows, giving the initial shape of a sine wave and no initial velocity:

$$\begin{aligned} \nu(x, 0) &= \nu_0 = 0.5 * \sin(x) \\ \frac{\partial \nu}{\partial t}(x, 0) &= \nu_1 = 0 \end{aligned}$$

A strand of hair was approximated as a hanging cable oriented horizontally. To shift the hanging cable to a horizontal orientation, it must be assumed that the hair is massless (and thereby not affected by gravity); this is a reasonable assumption for our approximation of a single strand of hair.

For the hanging cable representation of the strand, we use the governing equation:

$$\frac{\partial}{\partial \varphi} \left(\varphi \frac{\partial u}{\partial \varphi} \right) + S(\varphi, t) = \frac{1}{w^2} \frac{\partial u}{\partial t^2} \quad (2)$$

We apply a custom integral transform \mathcal{L} to u and the initial conditions, giving $\mathcal{L}\{u\} = \bar{u}_n$, $\mathcal{L}\{u_0\} = \bar{u}_{n,0}$, $\mathcal{L}\{u_1\} = \bar{u}_{n,1}$, and $\mathcal{L}\{S\} = \bar{S}_n$. With the use of \mathcal{L} and the Laplace transform, we come to the solution for $u(\varphi, t)$ (see details in Appendix B):

$$u(\varphi, t) = \sum_{n=1}^{\infty} \bar{u}_n(t) \frac{y_n(\varphi)}{\|y_n\|^2} \quad (3)$$

With

$$\begin{aligned} \bar{u}_n(t) &= \frac{L w y'_n(L)}{\mu_n} \int_0^t f_L(t - \tau) \sin(w \mu_n \tau) d\tau \\ &\quad - \frac{w}{\mu_n} \int_0^t \bar{S}_n(t - \tau) \sin(w \mu_n \tau) d\tau \\ &\quad + \bar{u}_{n,0} \cos(w \mu_n t) + \frac{\bar{u}_{n,1}}{w \mu_n} \sin(w \mu_n t) \end{aligned} \quad (4)$$

We couple the systems by bounding the hanging cable on one end to the wave equation. We do this by setting the hanging cable's boundary condition at $\varphi = L$ as follows:

$$u(L, t) = f_L(t) = \nu(x_0, t) \quad (5)$$

at a point x_0 along the wave's domain, which we call the anchor point.

We set the rest of the conditions and parameters as follows: $L = 1$, $w = 1$, $u(\varphi, 0) = u_0(\varphi) = L - \varphi - \nu(x_0, 0)$, and $S(\varphi, t) = 0$. The boundary condition implemented at $\varphi = 0$ was that of a free end, with $u(0, t) < \infty$, allowing the motion of this end to be determined entirely by the reaction of the strand to the coupled boundary condition at $\varphi = L$.

To visualize the wave and cable together, we shift the spatial domain of the cable to align the boundary point with the anchor point on the wave. This is accomplished by plotting the cable parametrically and shifting the x component by $-1 + x_0(t)$, giving $x = \varphi - 1 + x_0(t)$.

Variations

We experimented with several variations in parameters and coupling schemes, which yielded interesting results. We compared the behavior of several hanging cables bounded at different anchor points (see Figure 1).

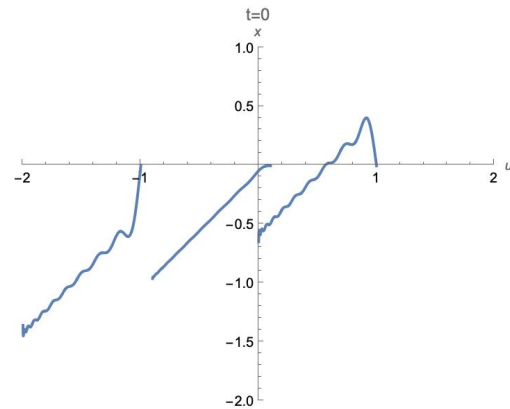


Figure 1: Three cables in simulation, spaced approximately evenly at $x_0 = \{-1, 0.1, 1\}$ and bounded by the wave equation on one end. This frame shows the initial state at $t = 0$.

We also visualized coupling the hanging cable using the wave equation as a source function instead of a boundary condition. For that setup, we included several point sources in the sourcing function based on the value of the 'wind' wave at that point; the discretization of the wave equation for use as a source function was done as implementing the full wave equation as a source function was computationally expensive. We left one end of the cable bounded to a single stationary point and observed the behavior resulting from the source function. For example, one sourcing function we used was

$$S(\varphi, t) = \sum_{k=0}^j S_0 \delta \left(\varphi - \frac{k}{j} * L \right) \nu \left(\frac{k}{j} * L, t \right) \quad (6)$$

This sourcing equation includes $j \in \mathbb{Z}_+$ point sources, with magnifying factor S_0 .

Results

We found that a hanging cable bounded on one end to an infinite wave equation produces visually compelling results. Given the length of the cable, the bounded end is pulled in the direction of the wave while the free end is often tending in the other direction. The delay of propagation across the cable, along with the sinusoidal behavior at the bounded end, often creates curves along the cable, as seen in Figure 2.

We observed that in the bounded cable simulations, the bounded end of the cable at $\varphi = L$ always stayed at $u = 0$, despite being bounded by $f_L(t) = \nu(x_0, t)$. We believe that this behavior can be explained by our use of finite series to approximate the infinite series in the inverse transform of \bar{u}_n .

While the hanging cable we analyzed was not a physical model of hair, the reaction of the cable to being bounded by the wave function is reminiscent of a strand of hair—perhaps a strand of hair in a horse's tail. In Figure 4, it can be seen that the strands of hair react differently to the motion of the horse combined with the fluid flow of the air around the horse's body and across/along the tail and the flow of the surrounding strands. The individual strands in the tail have a wave-like shape due to the motion, and many appear similar to the shape seen for the hanging cable in Figure 2.

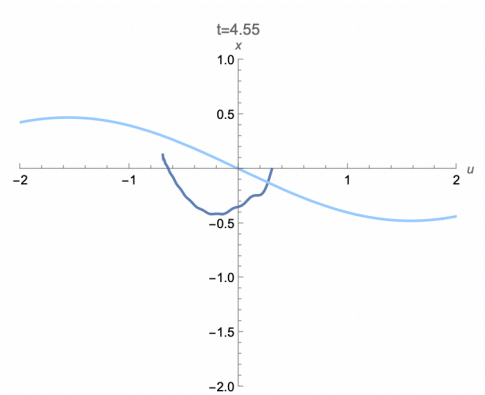


Figure 2: This frame is taken from the standard bounded setup given in this paper at simulation time $t = 4.55$. The bounded side of the curve on the right-hand side is pulled downward, while the left-hand end of the curve still points upward. Compare with Figure 4

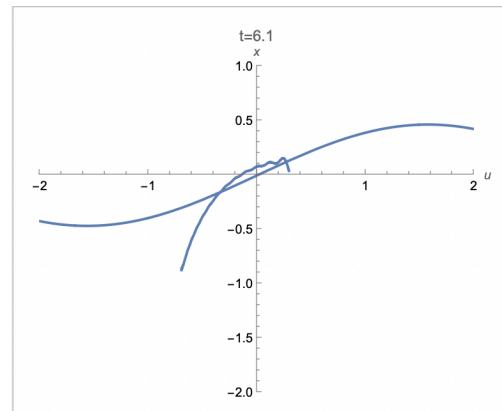


Figure 3: A frame of the wave-cable simulation at time $t = 6.1$. In this simulation, the cable's right end is bounded by the value of the wave.



Figure 4: A frame of a video of a horse galloping, taken from [4]. The general shape of the tail produces a curve.

Our forced variation, which uses point sources along the cable instead of bounding the cable to the wave, produced interesting results. As the cable is driven towards the wave at several points, resulting bumps in the cable are not limited to propagating from $\varphi = L$ to $\varphi = 0$ as in the bounded system. Instead, it occasionally propagates towards $\varphi = L$ as well, as is the case in Figure 5 and is best seen in the full animation.

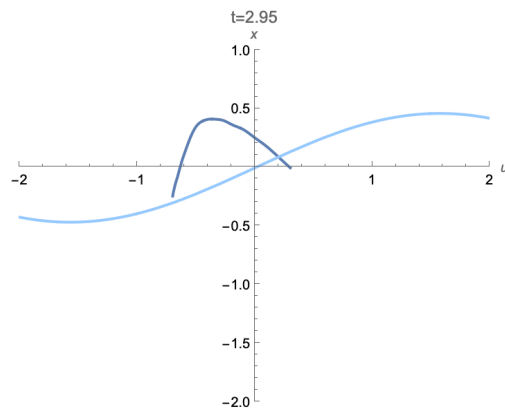


Figure 5: A frame of the sourced variation of our wave-cable simulation at time $t = 2.95$. In this simulation, one end of the cable is bounded at a fixed point and the cable is acted upon by five point sources along its spatial domain driven by the wave values. In this frame, the bump is traveling towards the right.

For full animated simulations, please see our Github repository.

Conclusions

We investigated coupling of the infinite wave and hanging cable models by bounding one end of the cable to the wave. We achieved visually interesting results, which are analogous to situations of a horizontally oriented cable-like structure being influenced by a wave-like medium. We suggest our system as an approximated model of hair moving in wind. The model does not reflect the physical properties of hair, but has visual similarities to the flowing of hair in wind.

Future work would include implementation of a more accurate physics-based model of the hair—for example, a discretized spring-mass system [1]—in order to better approximate the motion of the hair. Physical properties of the hair could be further implemented, especially insofar as they affect flow [3]. Additionally, the length of the hair was not held constant during this simulation; a more accurate simulation could be obtained through discretization in order to keep the hair length the same, or through calculation of the arc length and truncation to a given length at each time. The cable could also be treated as hanging vertically in addition to the implementation of physical parameters [2].

As mentioned previously in the paper, experimentation with implementing the wave equation as a forcing function required that it be discretized due high computational cost. Future work could also include more thorough implementation of the wave equation as a forcing function, whether through increasing the number of discrete forcing functions along the cable or by fully implementing the solution to the wave equation as a forcing function.

Acknowledgements

We would like to thank Dr. Soloviev and Tyler Stevens for their assistance with this project.

References

- [1] R. Fedkiw A. Selle M. Lentine. “A Mass Spring Model for Hair Simulation”. In: *ACM SIGGRAPH Conference Proceedings* (2008).

- [2] Michael Böhm et al. “Modeling and Boundary Control of a Hanging Cable Immersed in Water”. In: *Journal of Dynamic Systems, Measurement, and Control* (2014).
- [3] B.A. Batten B.T. Dickinson J.R. Singler. “Mathematical modeling and simulation of biologically inspired hair receptor arrays in laminar unsteady flow separation”. In: *Journal of Fluids and Structures* (2012).
- [4] BBC Earth. *Ultimate Horsepower in Super Slow Motion | BBC Earth Unplugged*. Youtube. 2013. URL: <https://youtu.be/86Zu8mqd8LM?t=110>.
- [5] Vladimir Soloviev. *Integrated Engineering Mathematics: A Comprehensive Review and Advanced Material for Graduate Students and Professionals*. 2024.

Appendix A Code

The following is the code used to make the primary visualization, written in Mathematica.

```
(*Make the 'sea' (infinite wave equation*)

sea[x_, t_] := (1/2)(sea0[x-v*t] +
  sea0[x + v*t]) +
  (1/(2*v)) *
  Integrate[seal[s], {s, x-v*t, x+v*t}]

v = 2
sea0[x_] := 0.5*Sin[x]
seal[x_] := 0

(*Animate 'sea' by itself*)
Animate[Plot[sea[x, t], {x, -5, 5},
  PlotRange->{{-5, 5},{-1, 1}},
  {t,0,5,0.1}]

(*Make the hanging cable*)
yn[x_, n_] := BesselJ[0, 2*mu[n]*Sqrt[x]]
ynnrm[x_, n_] :=
  L*BesselJ[0, 2*mu[n]*Sqrt[L]]^2
  + L*BesselJ[1, 2*mu[n]*Sqrt[L]]^2
mu[n_] := N[
  (1/2)*Sqrt[(BesselJZero[0, n])^2/L]]
```

```
un[t_, n_] :=
  (L*w*Derivative[1, 0][yn][L, n])/mu[n]*
  Integrate[f[t-t]*Sin[w*mu[n]*tau],
    {tau, 0, t}] -
  (w/mu[n]) *
  Integrate[Sn[t - tau, n]*Sin[w*mu[n]*
    tau], {tau, 0, t}] +
  un0[t, n]*Cos[w*mu[n]*t] +
  un1[t, n]/(w*mu[n])*Sin[w*mu[n]*t]

u[x_, t_] :=
  Total[
    Table[un[t, n]*yn[x, n]/ynnrm[x, n],
      {n, 1, 20}]
  ]

(*Set hanging cable parameters*)
L=1;
w=1;
u0[x_] := L - x - sea[anchor[0], 0]
u1[x_] := 0
S[x_, t_] := 0

Sn[t_, n_] := Integrate[
  S[xx, t]*yn[xx, n], {xx, 0, L}]
un0[t_, n_] := Integrate[
  u0[xx]*yn[xx, n], {xx, 0, L}]
un1[t_, n_] := Integrate[
  u1[xx]*yn[xx, n], {xx, 0, L}]

(*Set boundary condition to infinite wave at anchor point*)
anchor[t_] := .3
fl[t_] := sea[anchor[t], t]

(*Precompile*)
cf = Compile[{{x, _Real}, {t, _Real}},
  Evaluate[u[x, t]]]

(*Plot*)
pcable[t_] :=
  ParametricPlot[{phi - 1 + anchor[t],
    -cf[phi, t]}, {phi, 0, L - 0.01},
  PlotRange -> {{-2, 2}, {-2, 1}},
  PlotLabel ->
    StringJoin["t=", ToString@t],
  AxesLabel -> {u, x}]

psea[t_] :=
  Plot[sea[x, t], {x, -5, 5},
```

```
PlotRange -> {{-5, 5}, {-1, 1}}]

Animate[Show[pcable[t], psea[t]],
{t, 0, 10, 0.05}]
```

Appendix B Hanging Cable

Here we will list the derivation of the hanging cable equation in more detail. This derivation comes from [5], with some typo corrections.

The governing equation is

$$\frac{\partial}{\partial \varphi} \left(\varphi \frac{\partial u}{\partial \varphi} \right) + S(\varphi, t) = \frac{1}{w^2} \frac{\partial^2 u}{\partial t^2}$$

$$0 < \varphi < L, t > 0$$

With boundary conditions

$$u(0, t) < \infty \quad u(L, t) = f_L(t)$$

and initial conditions

$$u(\varphi, 0) = u_0(\varphi) \quad \frac{\partial}{\partial t} u(\varphi, 0) = u_1(\varphi)$$

We use a finite integral transform.

Step 1: Analyze Differential operator L

Consider the operator L applied to $y(\varphi)$ such that $Ly \equiv \frac{\partial}{\partial \varphi} \left(\varphi \frac{\partial y}{\partial \varphi} \right)$. In self adjoint form, which is given by

$$Ly(\varphi) = \frac{1}{p(\varphi)} [(ry')' + qy]$$

we find $p(\varphi) = 1$, $r = \varphi$, and $q = 0$.

Step 2: Supplemental Eigenvalue Problem

Consider the eigenvalue problem corresponding to the operator L .

$$Ly = \lambda y \quad y(0) < \infty$$

$$\frac{\partial}{\partial y} \left(\varphi \frac{\partial y}{\partial \varphi} \right) = \lambda y \quad y(L) = 0$$

Construct the Sturm-Liouville problem

$$(\varphi y')' + [0 + \lambda \cdot 1]y = 0$$

Let $\lambda = -\mu^2$, and expand the equation to

$$\varphi y'' + y' + \mu^2 y = 0$$

$$y'' + \frac{1}{\varphi} y' + \frac{\mu^2}{\varphi} y = 0$$

This satisfies the general Bessel equation with $m = 0$, $\alpha = 0$, $p = \frac{1}{2}$, $a = 2\mu$, and $v = 0$.

The solution takes the form

$$y(\varphi) = c_1 J_0(2\mu\sqrt{\varphi}) + c_2 Y_0(2\mu\sqrt{\varphi})$$

Since y is bounded at $\varphi = 0$ and Y_0 is unbounded at $\varphi = 0$, c_2 must be zero. Applying the other boundary condition, we have

$$y(L) = 0 = c_1 J_0(2\mu\sqrt{L})$$

c_1 must not be zero everywhere, so we find $J_0(2\mu_n\sqrt{L}) = 0$ to be the characteristic equation for μ_n . An equivalent form of this characteristic equation is $\frac{1}{2} \sqrt{\frac{1}{L}} J_0(\mu_n)^2 = 0$, which we will use to write the zeroes of the characteristic function in terms of the zeros of the function $J_0(\mu)$, since they are easier to work with in our mathematics software.

We come to the solution of the eigenvalue problem, and also solve for the norm $\|y_n(\varphi)\|^2 = \int_0^L J_0^2(2\mu_n\sqrt{\varphi}) d\varphi$.

$$\text{Eigenfunctions } y_n(\varphi) = J_0(2\mu_n\sqrt{\varphi})$$

$$\text{Characteristic Eq. for } \mu_n \quad \frac{1}{2} \sqrt{\frac{1}{L}} J_0(\mu_n)^2 = 0$$

$$\|y_n(\varphi)\|^2 = L J_0^2(2\mu_n\sqrt{L}) + L J_1^2(2\mu_n\sqrt{L})$$

Step 3: Finite Integral Transform Pair

Define the finite integral transform \mathcal{L} by

$$\mathcal{L}\{u(\varphi)\} = \bar{u}_n = (u, y_n) = \int_0^L u(\varphi) y_n(\varphi) d\varphi$$

The corresponding inverse transform is

$$\mathcal{L}^{-1}\{\bar{u}_n\} = u(x) = \sum_{n=1}^{\infty} \bar{u}_n \frac{y_n(\varphi)}{\|y_n\|^2}$$

Derive the operational property (more details in the textbook)

$$\mathcal{L}\left\{\frac{\partial}{\partial\varphi}\left(\varphi\frac{\partial u}{\partial\varphi}\right)\right\} = -Lf_L(t)y'_n(L) - \mu_n^2\bar{u}_n$$

Step 5: Apply the integral transform to the governing equation and initial conditions

Let barred variables (i.e. \bar{u}) represent functions transformed by \mathcal{L} ; that is, $\bar{u} = \mathcal{L}\{u(\varphi)\}$.

$$\begin{aligned} \mathcal{L}\left\{\frac{\partial}{\partial\varphi}\left(\varphi\frac{\partial u}{\partial\varphi}\right) + S(\varphi, t)\right\} &= \mathcal{L}\left\{\frac{1}{w^2}\frac{\partial^2 u}{\partial t^2}\right\} \\ -\mu_n^2\bar{u}_n - Lf_L(t)y'_n(L) + \bar{S}_n(t) &= \frac{1}{w^2}\frac{\partial}{\partial t}\bar{u}_n. \end{aligned}$$

Then, apply the Laplace transform $\ell\{f(t)\} = F(s)$:

$$\begin{aligned} \ell\{-\mu_n^2\bar{u}_n - Lf_L(t)y'_n(L) + \bar{S}_n(t)\} &= \ell\left\{\frac{1}{w^2}\frac{\partial}{\partial t}\bar{u}_n\right\} \\ -w^2\mu_n^2U_n - Lw^2y'_n(L)\ell\{f_L(t)\} + w^2\ell\{\bar{S}_n(t)\} &= s^2U_n - s\bar{u}_{n,0} - \bar{u}_{n,1} \end{aligned}$$

Solving for U_n and applying the inverse Laplace transform using the convolution theorem yields

$$\begin{aligned} \bar{u}_n(t) &= \frac{Lwy'_n(L)}{\mu_n} \int_0^t f_L(t-\tau)\sin(w\mu_n\tau) d\tau \\ &\quad - \frac{w}{\mu_n} \int_0^t \bar{S}_n(t-\tau)\sin(w\mu_n\tau) d\tau \quad (7) \\ &\quad + \bar{u}_{n,0}\cos(w\mu_nt) + \frac{\bar{u}_{n,1}}{w\mu_n}\sin(w\mu_nt) \end{aligned}$$

For further details, please refer to section IX.5.9 of the textbook.